Title
Validation of fast-ion D-alpha spectrum measurements during EAST neutral-beam heated plasmas

Journal
Review of Scientific Instruments, 87(11)

ISSN
0034-6748

Authors
Huang, J
Heidbrink, WW
von Hellermann, MG
et al.

Publication Date
2016-11-01

DOI
10.1063/1.4960308

Validation of fast-ion D-alpha spectrum measurements during EAST neutral-beam heated plasmas

J. Huang,[1,a)] W. W. Heidbrink,[2] M. G. von Hellermann,[3] L. Stagner,[2] C. R. Wu,[1] Y. M. Hou,[1] J. F. Chang,[1] S. Y. Ding,[1] Y. J. Chen,[1] Y. B. Zhu,[2] Z. Jin,[1] Z. Xu,[1] W. Gao,[1] J. F. Wang,[1] B. Lyu,[1] Q. Zang,[1] G. Q. Zhong,[1] L. Hu,[1] B. Wan,[1] and EAST team[1,b)]
[1]*Institute of Plasma Physics, Chinese Academy of Sciences, P.O. Box 1126, 230031 Hefei, Anhui, China*
[2]*University of California, Irvine, California 92697, USA*
[3]*Diagnostic Team, ITER Organization, Route de Vinon-sur-Verdon 13067 St. Paul Lez Durance, France*

(Presented 8 June 2016; received 3 June 2016; accepted 8 July 2016;
published online 6 September 2016)

To investigate the fast ion behavior, a fast ion D-alpha (FIDA) diagnostic system has been installed on EAST. Fast ion features can be inferred from the Doppler shifted spectrum of Balmer-alpha light from energetic hydrogenic atoms. This paper will focus on the validation of FIDA measurements performed using MHD-quiescent discharges in 2015 campaign. Two codes have been applied to calculate the D_α spectrum: one is a Monte Carlo code, Fortran 90 version FIDASIM, and the other is an analytical code, Simulation of Spectra (SOS). The predicted SOS fast-ion spectrum agrees well with the measurement; however, the level of fast-ion part from FIDASIM is lower. The discrepancy is possibly due to the difference between FIDASIM and SOS velocity distribution function. The details will be presented in the paper to primarily address comparisons of predicted and observed spectrum shapes/amplitudes. *Published by AIP Publishing.* [http://dx.doi.org/10.1063/1.4960308]

I. INTRODUCTION

In magnetic fusion devices, fast ions as the main source of heat and momentum can determine the efficiency of heating or current drive, and also possibly drive instabilities that can expel fast ions causing damage. The fast-ion distribution function is often essential to understand energetic ion transport and related instabilities. One of the powerful diagnostics of the fast-ion distribution is known as fast-ion D-alpha (FIDA),[1] based on charge-exchange between the injected neutral beam particles and the high energetic deuterium ions, which has been widely used in many magnetic devices.[2–8]

To investigate the fast ion behavior on EAST (Experimental Advanced Superconducting Tokamak), FIDA diagnostic system has been planned and built since 2014[9] with the diagnostic performance evaluated by an analytical code called simulation of spectra (SOS).[10] This paper will focus on the validation of FIDA measurements performed using MHD-quiescent discharges in 2015 campaign. To validate EAST FIDA spectrum measurements, two codes have been applied to calculate the D_α spectrum: one is SOS, and the other is fortran90 version FIDASIM Monte Carlo code[6,11] on the basis of the fast-ion distribution provided by the TRANSP/NUBEAM simulations.

The paper is organized as follows. The diagnostic details and experimental methods will be introduced in Sec. II. The measured spectrum description will be presented in Sec. III. Sec. IV will discuss the detailed comparisons of predicted and observed spectra.

II. DIAGNOSTIC SPECIFICATIONS AND EXPERIMENTAL METHODS

EAST is a fully superconducting tokamak experimental device. Both co-current and counter-current neutral beam injectors have been available, shown in Figure 1(a) top view and (b) poloidal view, which can produce 2-4 MW beam power with 50-80 keV beam energy. The favorable viewing ports for vertical and tangential geometry are shown in Figure 1(a), and the more tangential beam with tangency radius 1.26 m from the A port is viewed by FIDA technique, as a neutral probe beam for the CX interaction and the excitation of observable spectra. To measure the vicinity of D_α emission (656.1 nm), FLP-200 VPH (Volume Phase Holographic) Spectrograph system is applied from Bunkoukeik, with the grating of 2400 g/mm, F-number of 2, the focal length of 200 mm, coupled with DU-888 iXon3 from Andor instruments (1024 × 1024 pixels, 13 × 13 μm/pixel). With a demagnification of 2:1, the center wavelength is 655 nm and the pixel dispersion is approximately 0.033 nm/pixel with a spectral range of about 32.8 nm. The exposure time was set to 10 ms in this study, with the slit width 20 μm, corresponding to FWHM of the instrument function 0.074 nm. OD3 neutral density filter is used with width 2 nm, in the vicinity of 656.1 nm (D_α) and 670.8 nm (Li I) to attenuate both strong cold D_α line and Li I emission. In this paper, the vertical view along $r/a \sim -0.1$ at $R \sim 180$ cm shown in Figure 1(b) was chosen for the validation.

For the validation and verification of measurements against simulations, the analysed discharges are essentially

Note: Contributed paper, published as part of the Proceedings of the 21st Topical Conference on High-Temperature Plasma Diagnostics, Madison, Wisconsin, USA, June 2016.
[a)]Electronic mail: juan.huang@ipp.ac.cn
[b)]See Appendix of B. N. Wan *et al.*, Nucl. Fusion **55**, 104015 (2015).

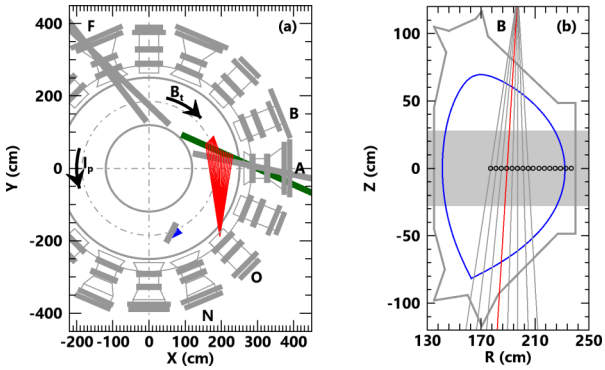

FIG. 1. (a) Top view and (b) poloidal view on the lines of sight setup of FIDA diagnostics on EAST.

free of MHD activity, allowing fast-ion transport in the neo-classical level. As shown in Figure 1(a), the L-mode discharge 55 408 had a counter-clockwise plasma current with 400 kA (Figure 2(a)), and a clockwise toroidal field with ~1.8 T on magnetic axis, a line averaged density of about 2.3×10^{19} m^{-3} (Figure 2(b)), and effective charge number $\langle Z_{eff} \rangle \sim 2.74$ obtained from visible bremsstrahlung diagnostic system. The electron density and temperature profile was provided by Thomson scattering diagnostics. The ion temperature profile was provided by crystal X-ray spectrometer. As shown in Figure 2(c), the D^0 probe beam ("A-port T") was modulated with 100 ms duration 10% duty cycle and produced 0.57 MW beam power, 47 keV beam energy with the measured power fraction about 75%:17%:8% for each full, half and third energy component. F-port tangential beam ("F-port T") produced 0.91 MW beam power, 55 keV beam energy with the measured power fraction of about 67%:26%:7%. The FIDA measurements during the second pulse are analyzed in this paper.

III. MEASURED FIDA SPECTRUM

Figure 3 shows the measured FIDA spectra. The absolute intensity calibration of FIDA measurements was done by tungsten ribbon lamps and further corrected by the corresponding visible bremsstrahlung measurements with the details discussed in Section IV. For the vertical view, both beam modulation and a paired passive view are available shown in Figure 1(a). A comparison between these two approaches shows good agreement in this MHD-quiescent shot. For passive impurity lines OV at 650.1 nm and OII at 664.1 nm, shown in Figure 3, with nearly no change comparing among "beam-on," "beam-off" and "passive," it shows that the plasma has a good temporal stationarity and verifies that the displaced reference view has a good toroidal symmetry with the active view. By background subtraction approaches, passive FIDA radiation can be eliminated to obtain active FIDA spectra shown as "net" in Figure 3. The passive oxygen lines disappear completely. Visible bremsstrahlung is also well subtracted, which is present in the FIDA spectra originating from the whole plasma and shows nearly a flat offset for a spectral feature, above the injection energy from the wings of the measured spectrum.

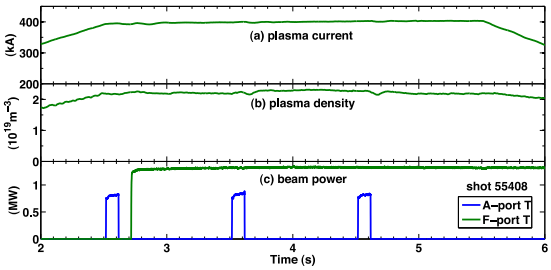

FIG. 2. Time traces of shot 55 408 including (a) plasma current, (b) the line averaged electron density, and (c) NBI heating power with F-port tangential beam and modulated A-port tangential beam.

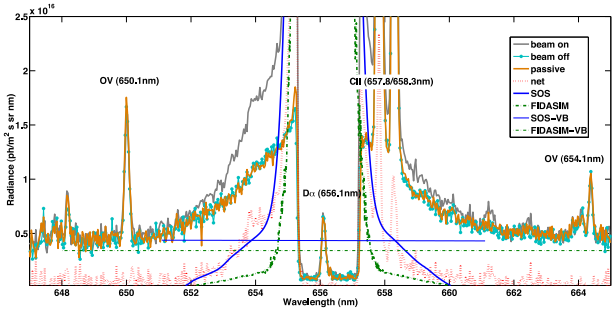

FIG. 3. The FIDA spectrum from a poloidal LOS at r/a ~ 0.1: (1) measured spectra: including both active and passive components during the probe beam on ("beam on"), passive spectra during the beam off ("beam off"), passive spectra from the pair N-port passive viewing ("passive"), active FIDA radiation ("net") with the subtraction of "beam off" from "beam on"; (2) calculated spectra: from SOS and FIDA simulations excluding bremsstrahlung part ("SOS," "FIDA"), and each bremsstrahlung calculations ("SOS-VB," "FIDA-VB").The intensity of the cold D_α line have been attenuated by the neutral density filter placed in the focal plane between the spectrometer and camera.

IV. COMPARISON AND DISCUSSION

Figure 3 shows the comparison between the measured and simulated spectra. The predicted SOS fast-ion spectrum agrees well with the measurement; however, the level of fast-ion part from FIDASIM is lower. The main components for calculated spectrum, shown in Figure 4, include the following: (1) the radiation from visible bremsstrahlung ("`VB continuum`"); (2) the emission from beam neutrals with full, half, and one third of injection energy ("`Beam emission`"); (3) the radiation

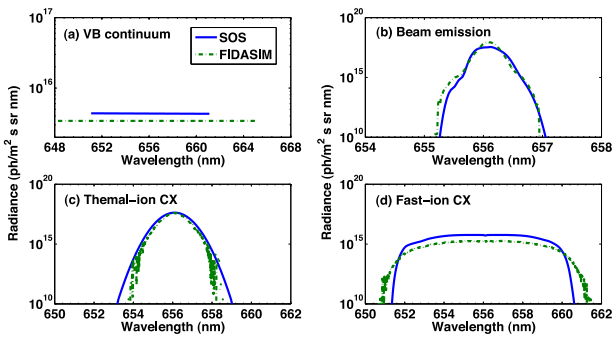

FIG. 4. Comparisons of each main part from SOS and FIDASIM: (a) VB continuum, (b) beam emission, (c) thermal-ion CX, and (d) fast-ion CX. Details are given in the text.

emitted by thermal/halo ions that undergo charge exchange reactions with beam neutrals ("Thermal-ion CX"); (4) the radiation emitted by neutralized fast ions ("Fast-ion CX"). In this paper, the primary objective is to validate FIDA measurements by addressing comparisons of predicted and observed shapes/amplitudes. The data consistency validation procedure will be discussed as the following steps.

The prediction of "VB continuum" level is a central issue in the quantitative spectroscopy evaluation process since it is a measurement of the common plasma, the torus and viewing geometry, and the absolute calibration of the spectroscopic instrumentation. Thus the first step is to check the consistency between the continuum measurements and the models. The measured VB continuum level at 523 nm is $\sim 3.26 \times 10^{15}$ ph/(m^2 s sr nm). In SOS, considering the viewing geometry and wavelength dependence, with the setting $\langle Z_{eff} \rangle \sim 2.74$, corresponding to impurity ion concentration $C^{+6}(5.6\%)$ and $Li^{+3}(1\%)$, the deviation is less than 5% between the measurement and calculation. In Figure 3(a), according to the near flat offset above the injection energy from the wings of the measured FIDA spectrum, the absolute calibration was corrected using plasma continuum radiation as calibration source with cross-calibration factor of about 1.75, because the collection optics might be degraded with the intensity calibration prior experimental campaign. In Figure 4(a), the deviation about 23% between SOS and FIDASIM "VB continuum" level is due to the different gaunt factors applied. SOS uses Burgess-Summers gaunt factor, while FIDASIM uses gaunt factor without wavelength dependence. When both codes use Burgess-Summers gaunt factor, the discrepancy is reduced to 9%. The "VB continuum" level comparison shows that the continuum model is consistent between the codes and the measurements.

The observed fast-ion feature is the result of the line of sight integration of the fast ion spectrum which is the product of source rate, effective cross sections, velocity distribution function, and local beam density, etc. Figure 4(b) shows the comparison of "Beam emission" part between SOS and FIDASIM. With same beam characteristics (power, energy, fractions, beam size, etc.), SOS calculation shows a good agreement with FIDASIM prediction with the matched shape. The observation geometry setting in FIDASIM code is corresponding to $r/a \sim -0.1$ in SOS modelling, which gives an exactly vertical view with no doppler shift of beam emission spectrum. Figure 4(c) shows the comparison of "Thermal-ion CX" part. FIDASIM thermal ion CX width and amplitude matches SOS predictions with the SOS doppler width corresponding to $T_i = 1.2$ eV. Both SOS "Beam emission" and "Thermal-ion CX" parts appear to agree with the corresponding FIDASIM predictions, indicating that local CX emission rate as well as halo effect agrees in SOS and FIDASIM modelling. However, in Figure 4(d) there is a discrepancy for "Fast-ion CX" part between these two codes; FIDASIM calculation is lower than SOS evaluation. The substantial differences between the two codes are that, compared with FIDASIM applying a multi-particle Monte Carlo code, the fast ion slowing-down function in SOS is the anisotropic function from the analytical solution of the Fokker-Planck neutral injection equation.[12] Thus, the most possible reason for the difference of "Fast-ion CX" part between two codes is the value for the on-axis source rates from A- and F-injector combined, that is, the neutral beam stopping calculation and the slowing-down velocity distribution functions.

ACKNOWLEDGMENTS

This is supported by National Natural Science Foundation of China Grant No. 11575249, National Magnetic Confinement Fusion Energy Research Program of China under Contract Nos. 2015GB110005, 2014GB109004, 2012GB101001, and JSPS-NRF-NSFC A3 Foresight Program in the field of Plasma Physics (NSFC No. 11261140328).

[1]W. W. Heidbrink, Rev. Sci. Instrum. **81**, 10D727 (2010).
[2]M. G. von Hellermann, W. G. F. Core, J. Frieling, L. D. Horton, R. W. T. Konig, and H. P. Summers, Plasma Phys. Control. Fusion **35**, 799 (1993).
[3]W. W. Heidbrink, K. H. Burrell, Y. Luo, N. A. Pablant, and E. Ruskov, Plasma Phys. Control. Fusion **46**, 1855 (2004).
[4]M. Podestà, W. W. Heidbrink, R. E. Bell, and R. Feder, Rev. Sci. Instrum. **79**, 10E521 (2008).
[5]E. Delabie, R. J. E. Jaspers, M. G. von Hellermann, S. K. Nielsen, and O. Marchuk, Rev. Sci. Instrum. **79**, 10E522 (2008).
[6]B. Geiger, M. Garcia-Munoz, W. W. Heidbrink, R. M. McDermott, G. Tardini, R. Dux, R. Fischer, V. Igochine, and the ASDEX Upgrade Team, Plasma Phys. Control. Fusion **53**, 065010 (2011).
[7]M. Osakabe, S. Murakami, M. Yoshinuma, K. Ida, A. Whiteford, M. Goto, D. Kato, T. Kato, K. Nagaoka, T. Tokuzawa, Y. Takeiri, and O. Kaneko, Rev. Sci. Instrum. **79**, 10E519 (2008).
[8]C. A. Michael, N. Conway, B. Crowley, O. Jones, W. W. Heidbrink, S. Pinches, E. Braeken, R. Akers, C. Challis, M. Turnyanskiy, A. Patel, D. Muir, R. Gaffka, and S. Bailey, Plasma Phys. Control. Fusion **55**, 095007 (2013).
[9]J. Huang *et al.*, Rev. Sci. Instrum. **85**, 11E407 (2014).
[10]M. G. von Hellermann, E. Delabie, R. Jaspers, P. Lotte, and H. P. Summers, AIP Conf. Proc. **1058**, 187 (2008).
[11]W. W. Heidbrink, D. Liu, Y. Luo, E. Ruskov, and G. Geiger, Commun. Comput. Phys. **10**, 716 (2011).
[12]U. Gerstel, L. Horton, H. P. Summers, M. von Hellermann, and B. Wolle, Plasma Phys. Control. Fusion **39**, 737 (1997).